

Thomas W. Petrie,¹ Jan Kośny,² Jerald A. Atchley,³ and André O. Desjarlais⁴

Effect of Steel Framing in Attic/Ceiling Assemblies on Overall Thermal Resistance

Reference: Petrie, T. W., Kośny, J., Atchley, J. A., and Desjarlais, A. O., “**Effect of Steel Framing in Attic/Ceiling Assemblies on Overall Thermal Resistance,**” *Insulation Materials: Testing and Applications: Fourth Volume, ASTM STP 1426*, A. O. Desjarlais and R. R. Zarr, Eds., American Society for Testing and Materials, West Conshohocken, PA, 2002.

Abstract: Experiments have been performed to assess the impact of cold-formed-steel framing on the thermal performance of attic/ceiling assemblies. Test configurations duplicated features of full-sized, truss-based and conventional joist-and-rafter assemblies away from the edges of the ceiling. Steady-state tests were done at winter conditions in a climate simulator. In truss systems, strong thermal bridges due to framing members that penetrated through the insulation to the bottom chords persisted as the insulation level increased. Without penetrations, the effect of steel framing eventually disappeared as insulation level was increased. For negligible effect of the framing, framing spaced 41 cm oc required greater insulation depth than did framing spaced 61 cm oc. Without penetrations but with enough insulation to cover framing with depths of 8.9 cm, 20.3 cm and 30.5 cm, greater framing depth yielded slightly poorer thermal performance. In some tests, a continuous layer of extruded polystyrene foam insulation was placed between the C-shaped bottom chords of trusses and the gypsum board ceiling. System R-values improved slightly more than the R-value of the foam insulation. A three-dimensional model of the thermal behavior of the assemblies was used to extend the test results to the entire range of steel-framed attic/ceiling configurations. Equations generated from this and related work can be the basis for changes in codes and standards that reflect the effect of steel framing on the thermal performance of attic/ceiling assemblies and discourage allowing steel framing to extend beyond insulation in the assemblies.

Keywords: thermal bridges, steel framing, residential attics, hot box tests, system R-value, code support

¹⁻⁴ Research Engineer, Research Engineer, Research Support Staff Member and Group Leader, respectively, Engineering Science & Technology Division, Oak Ridge National Laboratory, Oak Ridge, TN.

Introduction

Cold-formed-steel framing (also called light-gauge-steel framing) in residential building envelopes has the potential to create more severe thermal bridges than does wood framing. The situation during steady-state heat transfer by conduction illustrates the potential problem. The rate of heat flow by conduction is directly proportional to the product of a material's thermal conductivity and its cross-sectional area perpendicular to the direction of heat flow. The thermal conductivity of steel is at least two orders of magnitude larger than that of wood. Smaller cross-sectional areas are possible for steel to support the same mechanical load as wood because of steel's higher mechanical strength. However, areas with steel are not two orders of magnitude smaller and do not offset the effect of steel's higher thermal conductivity. Intense heat flow per unit area is possible through steel if materials in series with the steel can support it.

The *ASHRAE Fundamentals Handbook* [1] summarizes methods for estimating the overall thermal resistance of one-dimensional building components without thermal bridges. Isothermal plane and parallel path methods are explained. The thermal performance of curtain-wall and stud-wall constructions containing metal is also addressed. For ceilings and roofs with wood framing, the thermal resistance of a ceiling can be obtained by techniques that apply to flat construction. The thermal resistance of ventilated attic spaces under pitched roofs is more complicated. Under winter conditions, the thermal resistance of the attic space is small. Under summer conditions, a table is presented for the effective resistance of the attic space that accounts for varying ventilation air temperature, air flow direction and rate, ceiling thermal resistance, roof or sol-air temperature and surface emittance. These methods are applied in current codes and standards.

The current *ASHRAE Fundamentals Handbook* does not address the overall thermal resistance of attic/ceiling assemblies with steel framing. Therefore, it is not surprising that current codes and standards do not address them either. The problem is that their thermal resistance cannot be estimated with confidence by procedures that work for wood framing because of the potential for more severe thermal bridges with steel framing. Techniques for steel-framed walls are also of doubtful accuracy when applied to steel-framed attic/ceiling assemblies. Conventional joist-and-rafter assemblies do not have the sandwich-like construction of wall assemblies. Insulation, not construction materials, usually covers the joists. In some cases, the joists may not be completely covered and severe thermal bridges are created across all the joists. A further complication happens occasionally in conventional assemblies and regularly in truss-based assemblies. Support braces attached to the joists or bottom chords penetrate the insulation. Each one creates a persistent thermal bridge because a highly thermally conducting element communicates directly with the attic air regardless of the level of insulation.

The Oak Ridge National Laboratory's Buildings Technology Center did steady-state tests and analysis of them from September 2000 through mid-February 2001. The objective of this project was to address the lack of any information on steel-framed attic/ceiling assemblies in current codes and standards. Results of the tests are presented. The tests provided data to validate a model of the thermal behavior of steel-framed attic/ceiling assemblies away from the edges. Direct comparisons between the experiments and model are presented. Codes and standards that address attic/ceiling

assemblies are the International Code Council's (ICC) International Energy Conservation Code (IECC), formerly the Model Energy Code (MEC), and the American Society of Heating, Refrigerating and Air-Conditioning Engineers, Inc.'s (ASHRAE) Standard 90.1, Energy Standard for Buildings Except Low-Rise Residential Buildings and Standard 90.2, Energy Efficient Design of New Low-Rise Residential Buildings. This paper concludes with presentation of simple but accurate relationships that will allow inclusion of information on steel-framed attic/ceiling assemblies in codes and standards.

Apparatus and Procedures

The tests were done in the Large Scale Climate Simulator (LSCS) at the Oak Ridge National Laboratory's Buildings Technology Center according to ASTM C1363, Standard Test Method for the Thermal Performance of Building Assemblies by Means of a Hot Box Apparatus. Attic/ceiling assemblies were constructed especially for the tests. The C-shaped steel framing from 1.9-mm-thick stock had 3.8-cm-wide flanges and was 8.9 cm, 20.3 cm or 30.5 cm deep. Gypsum board that was 1.27 cm thick formed the ceiling. Horizontal framing to which the gypsum was attached was spaced 41 cm oc or 61 cm oc. Various depths of full-width fiberglass batt insulation were placed in layers between and over the horizontal framing. Given the number of tests that were needed, fiberglass batts were a good choice over loose-fill material in terms of ease of removal and ability to be reinstalled quickly and to a consistent R-value. For a few tests, 2.5-cm-thick extruded polystyrene foam insulation with a nominal R-value of 0.88 m²·K/W was placed between the bottom flanges of the horizontal framing and the gypsum board ceiling.

In some of the tests with the 8.9-cm-deep joists and in all of the tests with 20.3-cm-deep and 30.5-cm-deep joists, only batt insulation was placed between and over the joists. These configurations simulated conventional joist-and-rafter designs. With the 8.9-cm-deep framing, tests were also done with one to nine pieces of the framing attached vertically to each piece of the horizontal framing. The pieces extended upward through the insulation. These configurations simulated typical steel truss designs.

Up to three layers of fiberglass batt insulation were used. Two of the layers had nominal thickness of 15.9 cm. The third layer had nominal thickness of 8.9 cm. Thermal conductivity from 0.046 to 0.048 W/(m·K) is a typical range for fiberglass at room temperature. By dividing thickness by thermal conductivity, the nominal R-value of the 15.9-cm-thick batt is 3.4 m²·K/W. The nominal R-value of the 8.9-cm-thick batt is 1.9 m²·K/W. The four configurations of insulation that were tested had nominal R-values of 3.4, 5.3, 6.7 and 8.6 m²·K/W.

The actual R-value of the fiberglass insulation for each layer in each test was produced from the average installed thickness and density and from the thermal conductivity as a function of mean temperature and density. Thickness and density were determined according to ASTM C167, Standard Test Methods for Thickness and Density of Blanket or Batt Thermal Insulations, and thermal conductivity according to ASTM C518, Standard Test Method for Steady-State Heat Flux Measurements and Thermal Transmission Properties by Means of the Heat Flow Meter Apparatus. Temperatures measured on the top and the bottom of each layer during the tests were averaged to yield its mean temperature. Installed thickness of a layer divided by its thermal conductivity at

test temperature yielded its R-value at test conditions. The effect of temperature on insulation R-value was particularly important in the tests with foam insulation on top of the ceiling. The foam insulation shielded the fiberglass insulation from 21°C conditions below the assemblies more than the gypsum alone did. Therefore, the mean temperature of the fiberglass insulation was lower and its R-value was higher in the tests with foam insulation than without foam insulation, adding to system R-value.

Figure 1 shows an example test configuration that simulated a truss. For each horizontal framing member under the nominal R-3.4 m²·K/W insulation, except the two at the outer edges of the test section, three truncated braces extend upward through the insulation. Spacing between horizontal members is 41 cm oc. The center 2.44 m x 2.44 m area of the test section is the area that is metered in the LSCS for heat flow through the attic/ceiling assembly. During a test, the cover boards leaning against the back wall of the LSCS were placed on top of the assembly on a frame that fit into the brackets around the perimeter of the assembly. The cover boards formed a 0.61-m-deep unventilated attic space above the insulation.



Figure 1. *Example truss test configuration with three truncated braces attached to each bottom chord. Chords are spaced 41 cm oc and braces penetrate the nominal R-3.4 m²·K/W insulation.*

For the results presented in this paper, air temperature in the chamber above the attic/ceiling assembly was held at -18°C. Air flowed over the top of the assembly at a velocity of 0.5 to 0.8 m/s. Air temperature in the attic space was a few degrees warmer. The attic space was sealed against ventilation. Air temperature in the metering chamber under the ceiling was 21°C and air passed over the bottom of the ceiling at a velocity of 0.8 to 0.9 m/s. Results are reported in terms of an air-to-air system R-value obtained by the formula:

$$R_{system} = \frac{A \cdot \Delta T}{Q} \quad (1)$$

where

R_{system} is the air-to-air R-value in units of m²·K/W,

A is the area of the ceiling through which heat flows out of the metering chamber. It is equal to the 5.95 m² opening of the metering chamber for thin specimens. Here it was increased by 8.5% to 10.6%, depending upon insulation R-value, to account for two-dimensional heat flow around the perimeter through the relatively thick insulation,

ΔT is the temperature difference between the air below the ceiling and the air above the insulation, in K or °C, and,

Q is the net heat flow out of the metering chamber, obtained from an energy balance on the metering chamber, in W.

The air handling system in the metering chamber of the LSCS includes a water-cooled cooling coil, an electric resistance heating coil and circulation fans to move air over them. The ability to use cooling in the metering chamber is a unique feature that allowed us to test over the wide range of insulation R-values given above. For some tests, the heat added to the metering chamber by the fans was more than the heat flow out through the ceiling. Even at severe winter conditions, additional cooling was necessary to do the tests at the desired 21°C in the metering chamber. If cooling is sufficient, temperature control is done with the fast-responding electric resistance heating coil.

Measurement of the amount of cooling, Q_{cool} , is difficult over a long series of tests due to very slow drift in the calibration of the instrumentation used to sense the cooling water flow rate and its temperature rise when it flows through the metering chamber. For several cases in which net heat flow out of the metering chamber was sufficient for control without metering chamber cooling, tests were done with and without cooling to establish the appropriate correction, ΔQ_{cool} , for the metering chamber energy balance. The correction varied from a minimum of 6.8 W at the start of the tests to a maximum of 13.6 W near the end of the tests. The correction was 7% to 29% of the net heat flow.

With no cooling in the metering chamber, the bias and precision of the LSCS was established and has been checked periodically with a calibration panel fabricated from a 10.2-cm-thick piece of expanded polystyrene foam insulation. Figure 2 shows results from 1990 through 2001 with no cooling in the metering chamber (solid symbols). Also shown are results from 1998 through 2001 since cooling has been available in the metering chamber (open symbols). The fit of the data with no cooling and the limits of the 95% confidence interval about these data have been extended to the range of mean calibration panel temperatures when cooling was needed in the metering chamber. When net heat flow into the metering chamber was greater than 45 W, the amount of cooling was corrected with a linear function of the net heat flow to produce the R-values shown as the open symbols. As evidence of the goodness of this correction, note the distribution of these corrected R-values about the solid line. They fall generally within the limits of the 95% confidence interval that is shown by the dashed lines: $\pm 1.8\%$ to $\pm 2.3\%$ of the expected R-value [2]. Our experience with other test sections with higher R-value than the calibration panel is that uncertainty doubles as R-value doubles.

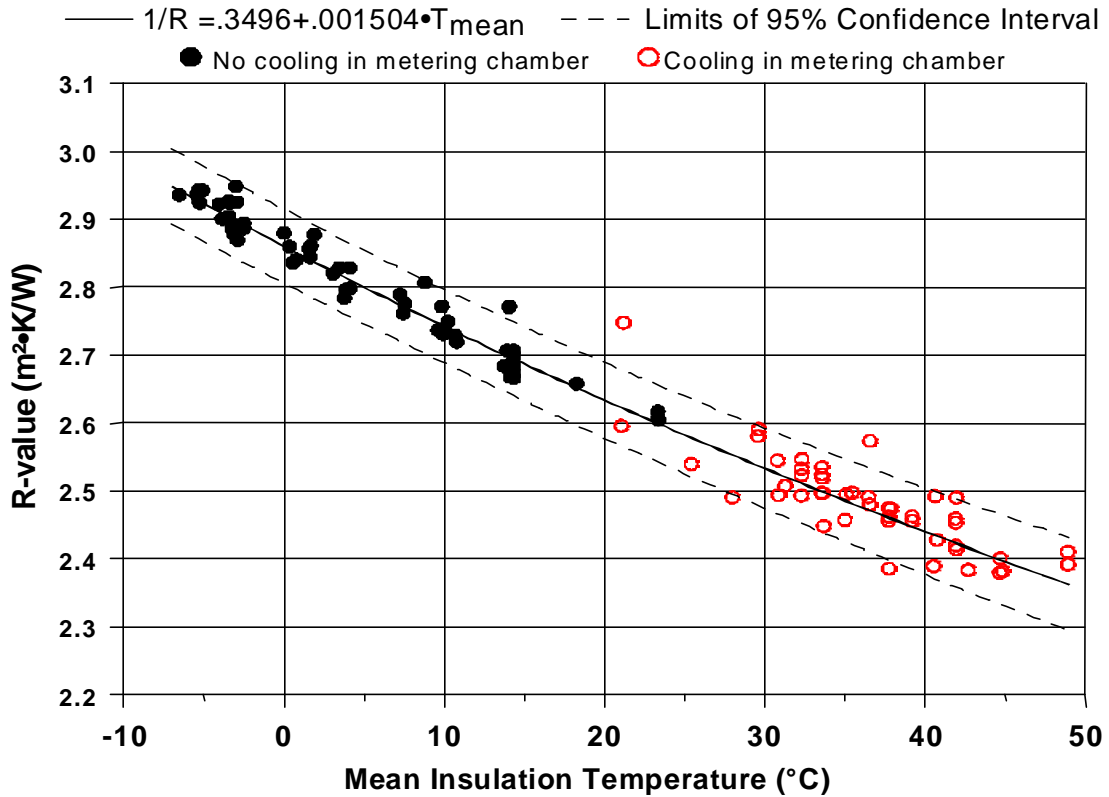


Figure 2. Results with a calibration panel to monitor the bias and precision of the Large Scale Climate Simulator.

Test Results and Discussion

Two working graphs have been prepared from the results with air temperature above the attic/ceiling assemblies at -18°C and air temperature below the ceiling at 21°C . Actual insulation R-values are used in the abscissas while system R-values as determined from Eq 1 are used in the ordinates. The graphs show trends in the experimental results that should be reflected in the model. They also show how internally consistent the test results are. This is of special concern because of the handling of the fiberglass batts from test to test that was required to change configurations in a timely manner.

Figure 3 shows the system U-value as a function of insulation U-value for tests with 8.9-cm-deep framing and various numbers of support braces to simulate trusses. U-value is the inverse of R-value. It is useful in this figure because the origin for insulation U-value represents infinitely thick insulation. Plotting U-values clearly shows how close the behavior is to that of insulation without any effects of steel framing. This situation is the bold line labeled No Steel in the figure. Solid symbols and light solid curves depict results for framing spaced 61 cm oc. Open symbols and light dashed curves show results for framing spaced 41 cm oc. Curves were hand drawn with a French curve through the data for each framing configuration that was tested at several insulation depths.

The configurations with 0 braces are expected to behave like framing-free assemblies as U-value approaches 0 (thick insulation depth). The assemblies with both 61 cm oc and 41 cm oc spacing of framing have this behavior. Performance for large

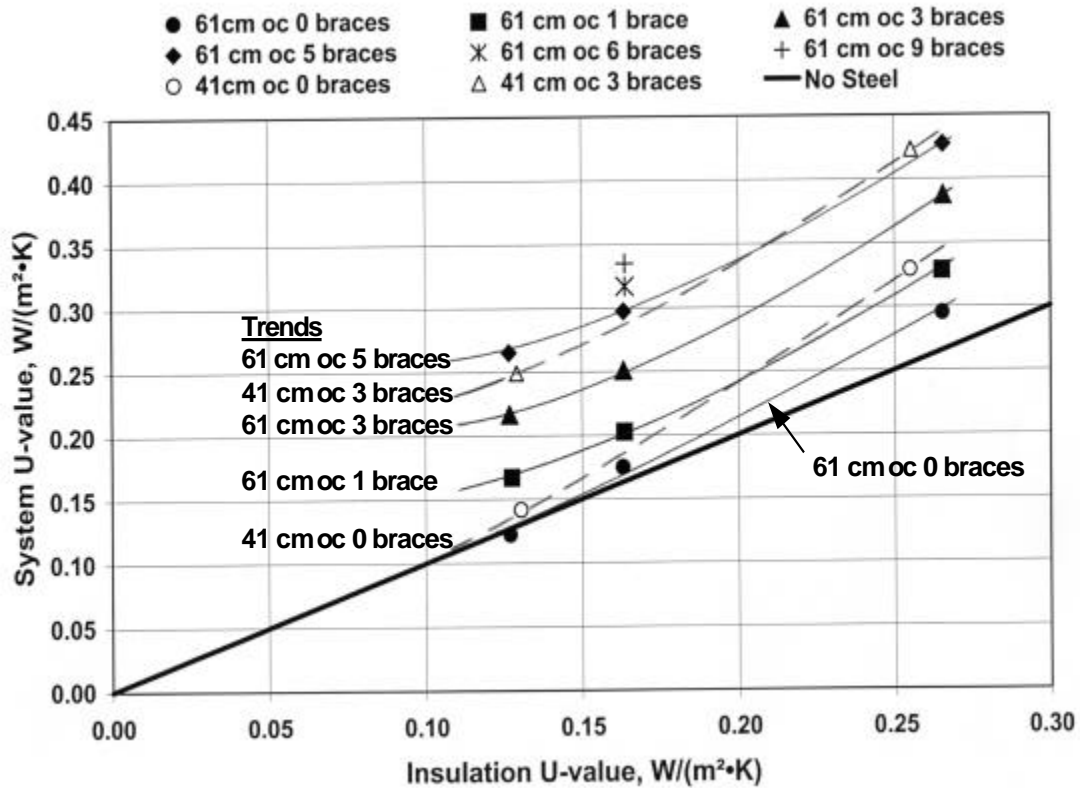


Figure 3. Test results and trends for simulations of steel trusses with various numbers of support braces.

insulation U-values (thin insulation depth) is worse for the 41 cm oc spacing than for the 61 cm oc spacing because 41 cm oc spacing causes more thermal bridges per unit area than 61 cm oc spacing. This is true for 0 braces and especially for 3 braces. Similarly, as the number of braces increases with framing spaced 61 cm oc, there are more thermal bridges per unit area of test section. Therefore, the curves and points for progressively more braces show progressively higher system U-values.

All braces were attached to the horizontal member that supported them within ± 0.9 m of length from the center of the horizontal member. Thus, all attachments were within the 2.44 m x 2.44 m metered area for Eq 1. For framing spaced 61 cm oc, the increase in system U-value from 6 to 9 braces is no more than the increase from 5 to 6 braces. This indicates that the thermal bridge caused by each of the 9 braces is not as severe as it is for each of the 6 braces. The thermal bridges are interfering with one another.

The braces extended upward through the insulation as shown in Fig. 1. Cold-formed-steel members penetrating from the attic air space through to the bottom chords will continue to cause thermal bridges no matter what the depth of insulation. The data in Fig. 3 with 1, 3 and 5 braces and framing spaced 61 cm oc suggest that the effect of these thermal bridges eventually dominates. If so, the curves for braces should become parallel to the abscissa, not the No Steel line, as insulation U-value approaches 0.

Figure 3 does not show the results of three tests in which a continuous layer of extruded polystyrene foam insulation having nominal R-value of $0.88 \text{ m}^2\cdot\text{K}/\text{W}$ was placed between the ceiling and the bottom chords. Nominal R-5.3 fiberglass batt

insulation was between each pair of bottom chords. The framing was spaced 61 cm oc. No braces, 1 brace and 5 braces penetrated the fiberglass insulation in the tests. There was relatively little thermal bridging in the tests with no braces and 1 brace, but the foam insulation did add its R-value to the system R-value. System R-value also increased (system U-value decreased) a small amount because the fiberglass insulation was colder when it was above the foam insulation and gypsum than when it was above the gypsum only. Because the continuous layer of foam insulation broke the many thermal bridges, it significantly improved the results with 5 braces. U-value with the foam insulation under this assembly fell on the curve drawn in Fig. 3 for framing 61 cm oc with 3 braces.

Figure 4 displays all data from tests without braces and includes results for framing with depths of 8.9 cm, 20.3 cm and 30.5 cm. There are two cases with three tests each that allow observation of trends. If system R-value is indeed linear with insulation R-value for each case, scatter is greater for 8.9-cm-deep framing spaced 61 cm oc than for 20.3-cm-deep framing spaced 41 cm oc relative to straight lines through the data for each case. The deviation from the line for the data with 8.9-cm-deep framing is at most $-0.26 \text{ m}^2\cdot\text{K}/\text{W}$ at system R-value of 5.7. This is within $\pm 5\%$ of R-5.7, where $\pm 5\%$ is the uncertainty expected at this level of R-value in the Large Scale Climate Simulator. Uncertainty masks whether or not system R-value is linear with insulation R-value.

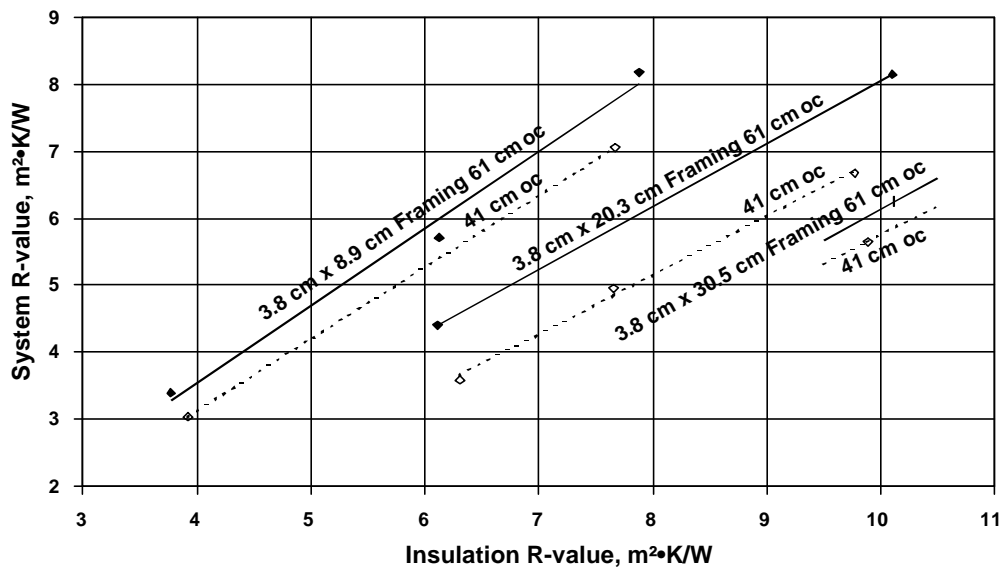


Figure 4. Test results and trends for simulations of steel-framed joist-and-rafter constructions.

When results for framing with depths of 8.9 cm, 20.3 cm and 30.5 cm are compared at about the same insulation R-values, the deeper the framing the lower the system R-value. Separation between the straight lines drawn through the data for framing spaced 61 cm oc and 41 cm oc is less for 8.9-cm-deep framing and 30.5-cm-deep framing than it is for 20.3-cm-deep framing. The slopes of the lines for the 20.3-cm-deep framing were used to draw lines through the data with 30.5-cm-deep framing. Differences in slopes among the three framing depths and two spacings are within expected uncertainty. The slight inconsistency in spacing is further discussed in the next section.

Development and Validation of the Computer Model

A finite difference computer code HEATING 7.3 [3] was utilized to model sections of steel-framed truss-based and conventional joist-and-rafter attic/ceiling assemblies. The model enabled data to be generated directly from principles of heat transfer for all steel-framed attic/ceiling configurations of interest without the need to interpolate or extrapolate experimental results. Trends that occur as parameters are varied are not subject to experimental uncertainty. In this paper, HEATING results represent “ideal” installation of insulation wherein no gaps exist between insulation and framing. In the field, some gaps will exist with all insulation products. The simulation results give maximum credit for the thermal insulation used in all configurations.

HEATING 7.3 is a multidimensional, general-purpose heat transfer code. Models in it may include multiple materials. The thermal conductivity, density, and specific heat of each material may be both time-dependent and temperature-dependent. Constant properties were used herein but they varied with the type of material and, for validation of the model, with the mean temperature of each layer of fiberglass batt insulation. Experimental values were used for the mean temperatures. HEATING allows boundary conditions that are known temperatures or any combination of prescribed heat flux, forced convection, natural convection, and radiation. For this paper, constant air temperatures were imposed at boundaries with solid materials. Constant values of heat transfer coefficients acted between solid materials and surrounding air.

Computer simulations of conventional joist-and-rafter attic/ceiling configurations were done for framing spaced 41cm oc and 61 cm oc. The joists with various depths were located in the middle of each section. In several cases where insulation with nominal R-values of 3.4 and 5.3 m²·K/W was used, steel was exposed above the top layer of fiberglass batts. The area exposed to the air, including both sides of the top flange, caused a severe thermal bridge through the assembly.

In the case of roof trusses, two models were used. One was the same as the conventional joist-and-rafter model for 61 cm oc spacing. In it, 1.22-m-long by 0.61-m-wide sections had only insulation and a steel bottom chord. In the other, 1.22-m-long by 0.61-m-wide sections of attic/ceiling assemblies also contained one, two or three vertical braces. The overall R-value of the truss assemblies was calculated by the following:

$$\frac{1}{R_{overall}} = \frac{f_{nb}}{R_{nb}} + \sum_i \frac{f_{b_i}}{R_{b_i}} \quad (2)$$

where

f_{nb} is the fraction of ceiling area occupied by the non-braced portion of the assembly,

R_{nb} is the R-value of the non-braced portion of the assembly from HEATING,

f_{b_i} is the fraction of ceiling area occupied by each braced portion of the assembly ($i = 1, 2, 3$ for one, two or three braces, respectively), and,

R_{b_i} is the R-value of the each braced portion of the assembly from HEATING.

Very detailed modeling was used to accurately account for the thermal influence of the steel framing, especially the vertical braces. Figure 5 shows, for insulation with R-value of 5.3 m²·K/W and a single brace extending vertically from the bottom chord, typical temperature variations throughout the 1.22-m-long by 0.61-m-wide section. For one vertical steel brace, as well as two and three vertical steel braces, the zone wherein

temperatures are disturbed by the braces is smaller than ± 0.61 m along the truss from the brace. The 1.22-m-long components used for modeling are long enough that the zones of disturbance from thermal bridges due to braces in adjacent components do not overlap. Therefore, parallel-path R-value calculations are justified for the overall R-value of steel-framed truss assemblies comprised of 1.22-m-long components. The parallel-path approximation is not valid within the components.

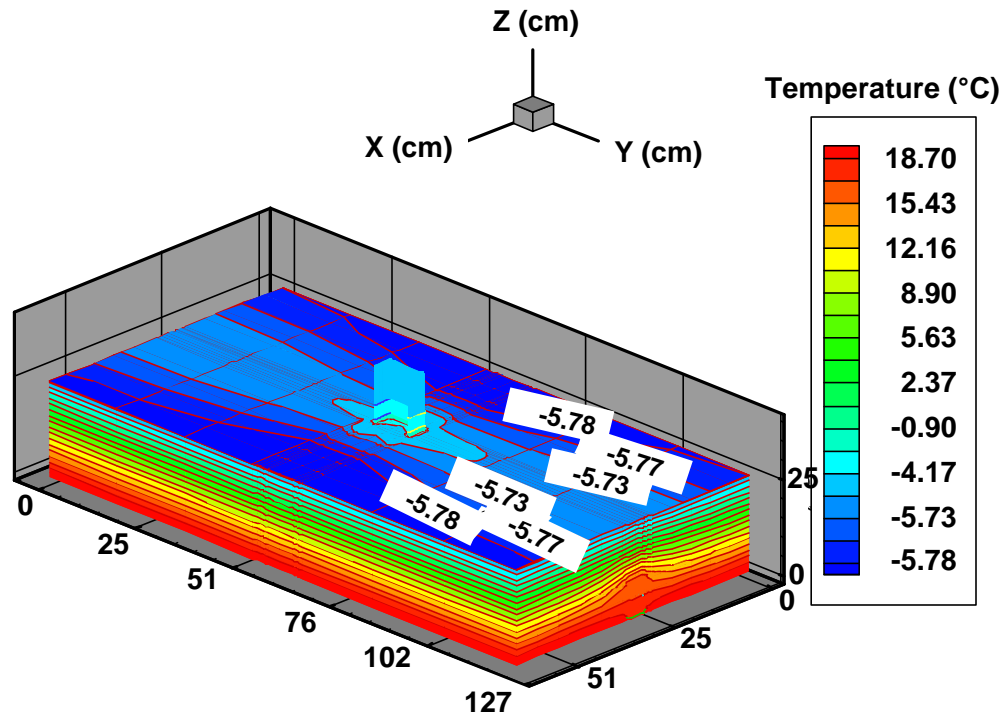


Figure 5. Detailed temperatures from model of 1.22 m x 0.61 m section of truss with 1 brace penetrating R-5.3 $m^2 \cdot K/W$ insulation.

No attempt was made to model the effect of any small gaps between the insulation and framing. Results from the model with no gaps between insulation and framing were compared with results from measurements with as-installed fiberglass batt insulation. See Figs. 6, 7 and 8. It was apparent from these comparisons that uncertainty in the test data masked any effects of the small gaps where the insulation did not conform exactly to the C-shaped steel framing members.

Figures 6, 7 and 8 provide evidence that the model is accurate and produces correct trends as parameters are varied. Direct comparison is made to results at the winter conditions of the tests. Mean insulation temperatures from our ASTM C1363 tests were available for the nominal 8.9-cm-thick layer and the two 15.9-cm-thick layers that were used in the various configurations. Apparent thermal conductivity at these temperatures from our ASTM C518 measurements was imposed in the model.

Figure 6 compares results from the model and the experiments for a simple truss system with one king post in the middle of the span. The comparison is done for the range of insulation R-values from the tests. This is the only truss system that we

simulated experimentally for which there was no doubt that zones of thermal disturbance from vertical braces were inside the metered area and did not overlap. Five spans from 2.4 m to 4.9 m were modeled. Spacing between trusses was 61 cm oc. In the model, these systems are combinations of two components. One is 1.2 m long and has a single vertical brace and R-value equal to R_{b1} . The other is long enough to complete the span and has no vertical braces and R-value equal to R_{nb} . R-value for each component was combined with its respective fractional area for each span using Eq 2.

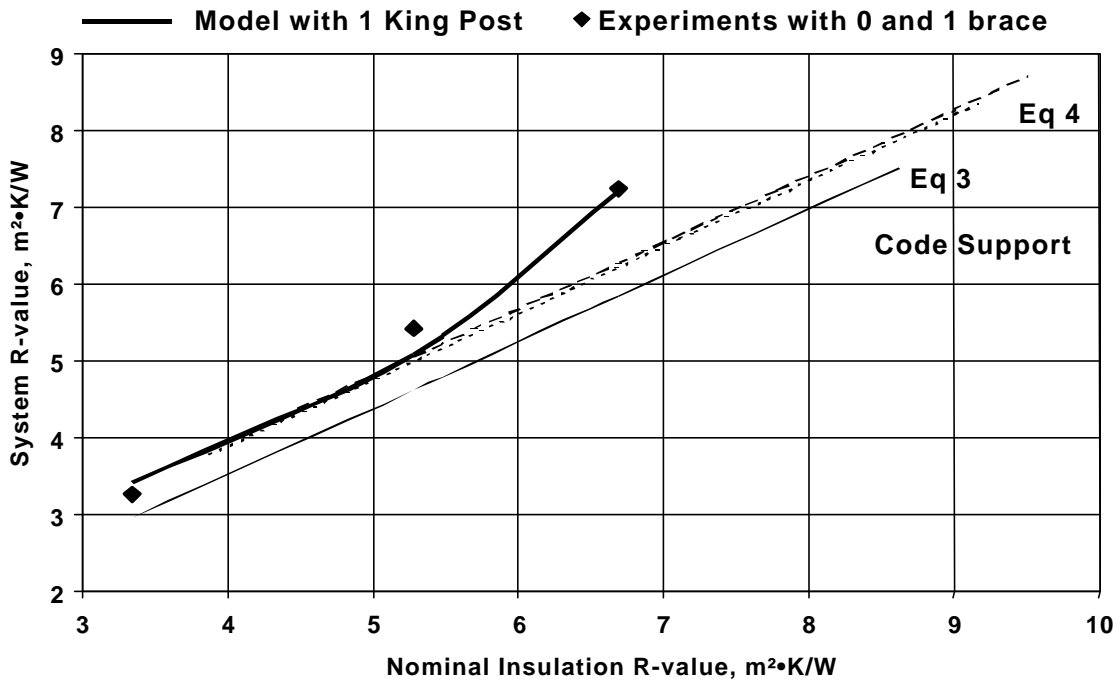


Figure 6. Comparison of truss system air-to-air R-values averaged over all spans from the experiments and the model with 1 king post.

The heavy solid curve in Fig. 6 shows the average for all spans from the model. System R-value is less than 2% higher for the longest span and less than 3% lower for the shortest span. The model was configured to yield the thermal resistance from the bottom of the ceiling to the top of the insulation including the effect of the framing. Thermal resistances of the air films measured in the experiments were added to yield the air-to-air system R-values shown for the model. The light lines labeled Code Support are explained in the next section after discussion of Eqs 3 and 4.

Results from the experiments with 8.9-cm-deep framing spaced 61 cm oc are shown as symbols in Fig. 6. The system R-values for the 61 cm oc 0 braces system in Fig. 3 were inserted directly for R_{nb} in Eq 2. The system R-values for the 61 cm oc 1 brace system in Fig. 3 were interpreted as $R_{overall}$ in Eq 2. Using the 0 brace experimental values as R_{nb} for a 1.2-m-long component with no braces, Eq 2 was solved for experimental values of R_{b1} for a 1.2-m-long component with one brace. These values of R_{nb} and R_{b1} were then used to estimate experimental R-values for the five spans with one king post. The average for all five spans at each insulation R-value is plotted.

Figure 6 shows that results from the model agree with the experiments within the uncertainty of measuring system R-values at high insulation R-values. It also shows that a model is very valuable for displaying correct trends when uncertainty masks their display from experiments. If a curve had been drawn on Fig. 6 through the experimental results, it would have shown almost linear increase of system R-value with nominal insulation R-value. We expect what the model shows, that the effect of the single king post on system R-value is less severe as insulation R-value increases. Therefore, system R-value should increase faster than insulation R-value.

Figures 7 and 8 display air-to-air system R-values for joists that are not thermally bridged by braces. Figure 7 is for 61 cm oc spacing and Fig. 8 is for 41 cm oc spacing. Solid symbols show experimental results from test sections wherein the joists were always covered by insulation. An additional open symbol in each figure is from results with an earlier test section constructed to support ASHRAE Technical Research Project 981 [4]. In that project, a few tests were done with joists not covered by insulation. That project also addressed effects of connections between joists, rafters and wall top plates.

Results from the model are shown as heavy curved lines in Figs. 7 and 8. For them, the sum of the thermal resistances of the air films above and below the assemblies was the average sum observed in the experiments. The lines are drawn smoothly through the air-to-air R-values that were predicted by the model at the four nominal insulation R-values for each joist depth. Thermal conductivity of the various layers was inserted at the mean temperature of each layer that was observed in the experiments. Modeled system

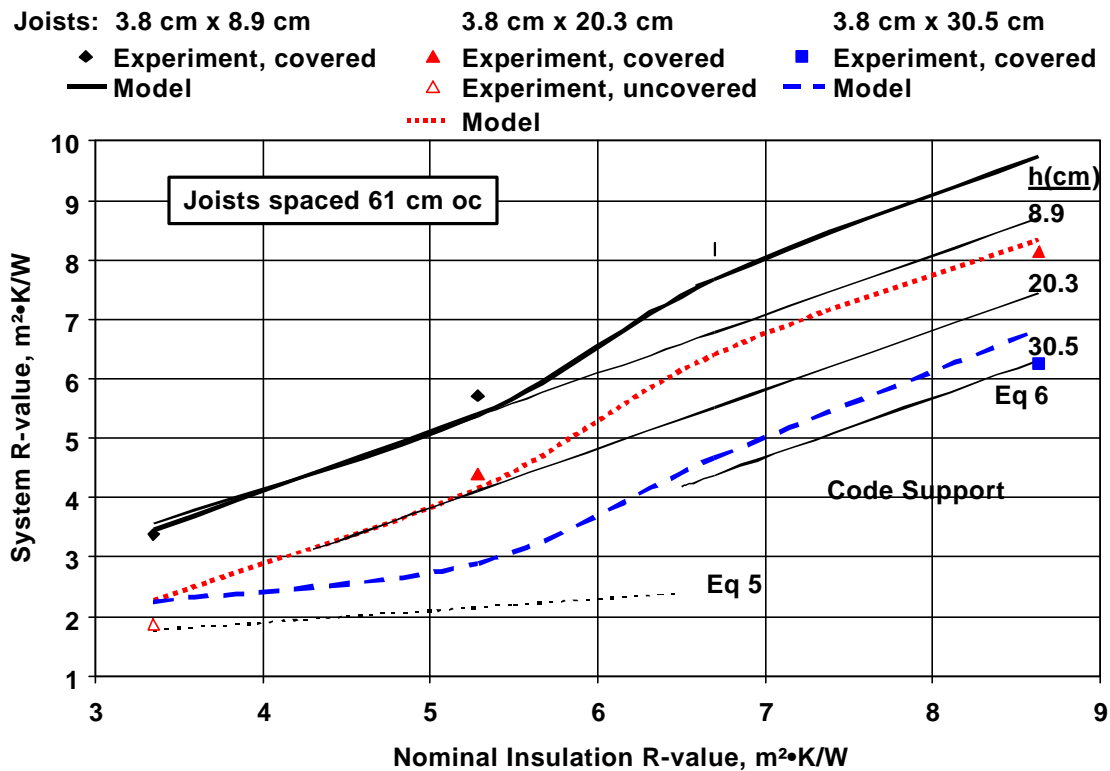


Figure 7. Comparison of experiment and model for conventional joist-and-rafter steel-framed assemblies with framing 61 cm oc.

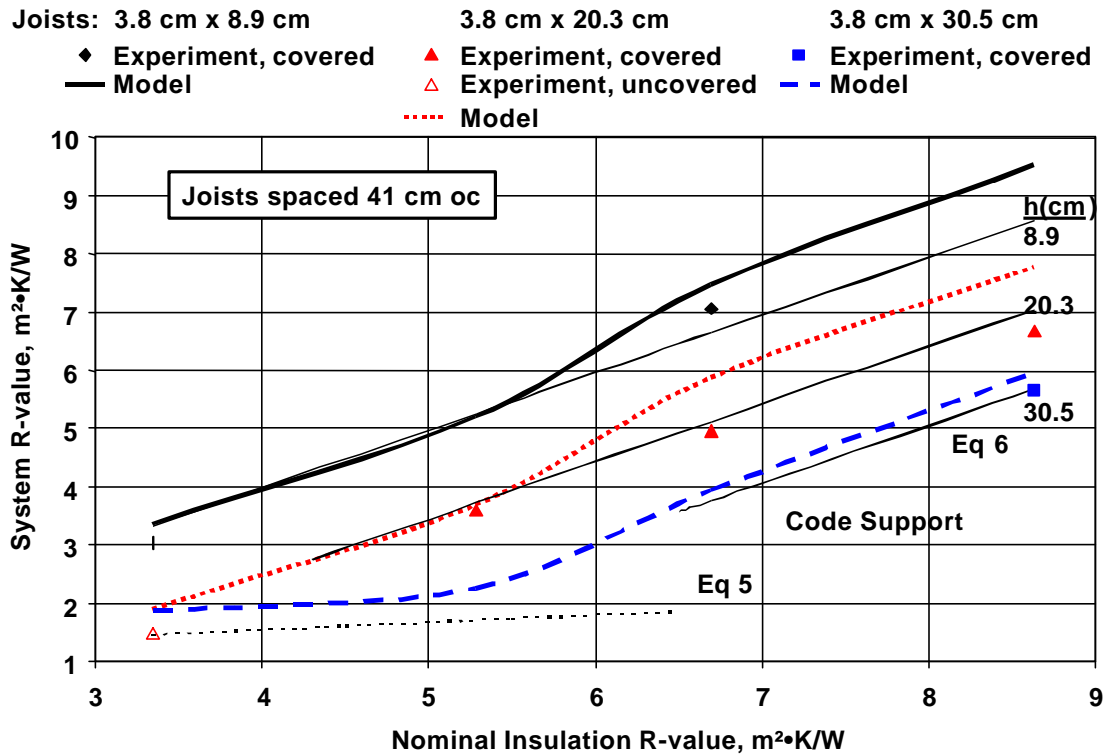


Figure 8. Comparison of experiment and model for conventional joist-and-rafter steel-framed assemblies with framing 41 cm oc.

R-values do not vary with nominal insulation R-value as smoothly as expected. However, as expected for a particular insulation thickness and framing depth, the modeled system R-values with framing spaced 41 cm oc are slightly smaller than with 61 cm oc. The light lines in Figs. 7 and 8 labeled Code Support are explained in the next section after discussion of Eq 5 for uncovered joists and Eq 6 for covered joists and the three framing depths, h .

In general, experimental values fall within experimental uncertainty above and below the appropriate curves from the model. The results with 20.3-cm-deep joists spaced 41 cm oc at the nominal insulation R-values of 6.7 and 8.6 $m^2 \cdot K/W$ are exceptions. Recall that data on Fig. 4 for the 20.3-cm-deep framing spaced 41 cm oc were not consistent with the rest of the data. System R-values for this case are far enough below model values in Fig. 8 to suspect flaws in the insulation configuration.

In the model, the insulation does not always cover completely the 20.3-cm-deep and 30.5-cm-deep framing. The top flange of the 20.3-cm-deep framing is above the R-3.4 insulation (with about 15.9 cm depth). The top flange of the 30.5-cm-deep framing is above both the R-3.4 insulation and the R-5.3 insulation (with about 24.8 cm depth). For uncovered joists, the model predicts a system R-value of about 2.3 $m^2 \cdot K/W$ for framing spaced 61 cm oc and about 1.9 $m^2 \cdot K/W$ for framing spaced 41 cm oc at a nominal R-value of 3.4 $m^2 \cdot K/W$. These values are slightly higher than the values obtained in the earlier project.

In summary, the system R-values from the model display the expected trends as the insulation R-value and framing configuration are varied. There are enough reliable

test results to confirm that the trends are correct. More importantly, there are enough reliable test results to ensure that system R-values from the model are accurate within experimental uncertainty.

Results with the Model for Support of Codes and Standards

Modeled configurations of attic/ceiling assemblies with steel framing were those that are likely to be built. Since assemblies in the field see both summer and winter conditions, properties were input at room temperature. We used 0.29 m²·K/W for the sum of air film thermal resistances and gypsum ceiling thermal resistance. The effect of going from winter to summer conditions is not large. For example, our ASTM C518 measurements on fiberglass batt insulation yielded nominal R-value of 3.4 m²·K/W at 24°C. They further showed that R-value of the insulation alone increased to R-3.8 at 4°C (winter conditions) and decreased to R-3.0 at 41°C (summer conditions). The effect of thermal bridges due to steel framing would not have much temperature dependence because the thermal conductivity of steel is very high relative to that of insulation at all temperatures. System R-values are expected to have less temperature dependence than insulation R-values, especially in highly thermally bridged situations.

We analyzed the results keeping in mind what is required to support development of codes and standards. For codes, simple relationships are needed that allow code officials to easily determine compliance. For standards, accurate relationships are needed to allow comparisons among alternatives and support energy efficient use of steel framing.

We addressed only truss systems made from 3.8 cm x 8.9 cm steel framing and installed 61 cm oc. The model showed that system R-value, within ±6%, was described for spans up to 15 m, with the appropriate number of braces, by an average over all spans. The number of support braces per unit length of span was such that thermal bridging did not vary much from the average situation.

We limited analysis of the effects of continuous extruded polystyrene foam insulation between the gypsum ceiling and the bottom chords to thickness from 1.3 cm to 2.5 cm. In this range, system R-value with foam insulation was 1.05 to 1.10 times the R-value of a system with the same amount of insulation R-value but with all of the insulation between and over the bottom chords. The continuous foam insulation made the extent of the thermal bridging slightly less severe in the fiberglass insulation. Temperature changes in the attic insulation due to the foam insulation and their effects on system R-value were neglected to approximate average behavior over all seasons.

The following equations describe air-to-air system R-values of truss systems made from 3.8 cm x 8.9 cm cold-formed-steel framing installed 61 cm oc. With no extruded polystyrene foam insulation between the ceiling and the bottom chords,

$$R_{\text{system}} = 0.864 \cdot R_{\text{insulation}} + 0.0581 \quad (3)$$

With 1.27 cm to 2.54 cm of foam insulation between the ceiling and bottom chords,

$$R_{\text{system}} = 0.864 \cdot R_{\text{insulation (including foam)}} + [0.36 + 0.050 \cdot t] \quad (4)$$

where

R_{system} is the air-to-air system R-value, in m²·K/W,

$R_{\text{insulation}}$ is the nominal insulation R-value, including R-value of the foam insulation if present between the ceiling and bottom chords of the trusses, in $\text{m}^2\cdot\text{K}/\text{W}$, and, t is the thickness of the foam insulation if present, in cm.

The system R-value from these equations is plotted in Fig. 6 against insulation R-value, including R-value of the foam insulation if present. Fiberglass insulation R-values were as high as $8.6 \text{ m}^2\cdot\text{K}/\text{W}$. Hence, insulation R-values for the equations extend to higher values than they do for the results of the truss tests and model validation on Fig. 6. The latter had lower depths of fiberglass insulation and no foam insulation. Equation 3 gives results that are conservative relative to results at winter conditions from the tests and model. This is desirable for year-round applications.

Two lines are shown for Eq 4. The short-dashed line is for 1.3-cm-thick foam insulation. The long-dashed line is for 2.5-cm-thick foam insulation. Thicker foam insulation does not improve system R-value very much at a particular value of total insulation R-value compared to the significant improvement from the situation with no foam insulation that is shown by the solid line for Eq 3. The 1.3-cm-thick foam insulation is thick enough to break the thermal bridges. Once continuous insulation breaks thermal bridges, more thickness adds little more than its R-value to the system R-value.

For conventional joist-and-rafter systems, 3.8-cm-wide steel framing with depths of 14.0 cm, 20.3 cm, 25.4 cm and 30.5 cm are of interest. We added 8.9-cm-deep framing because of its use for trusses. Spacings of interest are 41 cm, 49 cm and 61 cm oc. The usual situation is to cover the joists completely with insulation. However, it is possible that some attic applications call for joists that protrude beyond the insulation despite the severe thermal bridges that result when parts of the joists are exposed to attic air temperatures. This is a common situation for floors, for which parts of the joists are often exposed to more moderate basement or crawlspace air temperatures.

The need to address joists covered by insulation and joists not covered by insulation complicates development of codes and standards. The relationship between system R-value and insulation R-value is different for the covered and not covered situations. Also, a decision must be made about which situation is true for a particular application.

The amount of insulation that is installed is usually specified by R-value. In addition to R-value, the thermal conductivity or thermal resistivity is needed in order to estimate the installed thickness. For the fiberglass batt insulation used in the tests for this project, nominal thermal conductivity is $0.047 \text{ W}/(\text{m}\cdot\text{K})$. To cover an 8.9 cm-deep joist requires $R-1.9 \text{ m}^2\cdot\text{K}/\text{W}$. To cover a 20.3-cm-deep joist requires $R-4.3 \text{ m}^2\cdot\text{K}/\text{W}$. To cover a 30.5-cm-deep joist requires $R-6.5 \text{ m}^2\cdot\text{K}/\text{W}$.

The following equations describe air-to-air system R-values of conventional joist-and-rafter systems made from 3.8-cm-wide cold-formed-steel framing. Joist depth can range from 8.9 cm to 30.5 cm. Spacing can be from 41 cm oc to 61 cm oc. If the insulation thickness is such that parts of the joists are uncovered, the following relationship applies:

$$R_{\text{system}} = [0.00374 \cdot s - 0.028] \cdot R_{\text{insulation}} + [0.00295 \cdot s + 0.923] \quad (5)$$

If the insulation thickness is such that the joists are completely covered by insulation, then

$$R_{\text{system}} = 0.993 \cdot R_{\text{insulation}} + [0.00113 \cdot s - 0.180] \cdot h + [-0.00338 \cdot s + 1.333] \quad (6)$$

where

R_{system} is the air-to-air system R-value, in $\text{m}^2\cdot\text{K}/\text{W}$,

$R_{\text{insulation}}$ is the nominal R-value of the insulation, in $\text{m}^2\cdot\text{K}/\text{W}$,

s is the spacing between adjacent joists, in cm, and,

h is the depth of the joists, in cm.

Figures 7 and 8 include the straight lines that these equations produce when values for the relevant parameters are inserted. The dashed line for Eq 5 at all values of joist depth and the solid line for Eq 6 at joist depth of 30.5 cm that are drawn on both figures clearly illustrate the abrupt change in system R-value that is implied by these equations. A 30.5-cm-deep joist undergoes the transition from being uncovered to being covered near an insulation thickness corresponding to $R=6.5 \text{ m}^2\cdot\text{K}/\text{W}$ for the insulation used in the tests. The curve for the model of the 30.5-cm-deep joist was drawn smoothly between predictions made at the four nominal insulation R-values of 3.4, 5.3, 6.7 and $8.6 \text{ m}^2\cdot\text{K}/\text{W}$. Modeling for a typical case at additional R-values above and below the insulation R-value for the transition showed that the system R-value change is indeed gradual. Using the low values from Eq 5 should discourage the practice of exposing steel framing beyond insulation. The values from Eq 6 for covered joists at nominal conditions are conservative with respect to the modeled values at winter conditions with high levels of insulation. This is desirable for year-round applications.

Conclusions

Experiments have been performed to assess the impact of cold-formed-steel framing on the thermal performance of attic/ceiling assemblies. Test configurations duplicated features of full-sized, truss-based and conventional joist-and-rafter assemblies away from the edges of the ceiling. Steady-state tests were done at winter conditions in a climate simulator. In truss systems, strong thermal bridges due to framing members that penetrated through the insulation to the bottom chords persisted as the insulation level increased. Without penetrations, the effect of steel framing eventually disappeared as insulation level was increased. For negligible effect of the framing, framing spaced 41 cm oc required greater insulation depth than did framing spaced 61 cm oc. Without penetrations but with enough insulation to cover framing with depths of 8.9 cm, 20.3 cm and 30.5 cm, greater framing depth yielded slightly poorer thermal performance. A continuous layer of extruded polystyrene foam was placed between the C-shaped bottom chords of trusses and the gypsum board ceiling for a few tests. System R-values improved by slightly more than the R-value of the foam insulation.

A three-dimensional model of the thermal behavior of the assemblies was validated by direct comparison with the test results. Agreement between model and experiment was generally within experimental uncertainty. The model showed trends due to effects of parameter variations more consistently than the test data. The model allowed us to extend the test results to the entire range of cold-formed-steel-framed attic/ceiling configurations. Four linear equations were generated to summarize all results. Two reflected the behavior of truss systems with and without foam insulation between the ceiling and the bottom chords of the trusses. Two reflected the behavior of joist-and-rafter assemblies away from edges when the joists were not covered by insulation and when they were. The equations can be the basis for changes in codes and standards that

reflect the effect of steel framing on the thermal performance of attic/ceiling assemblies and discourage allowing steel framing to extend beyond the insulation.

Acknowledgment

This paper was prepared by the Buildings Technology Center at the Oak Ridge National Laboratory, Oak Ridge, Tennessee. The Oak Ridge National Laboratory is managed by UT-Battelle, LLC for the U.S. Department of Energy under contract No. DE-AC05-00OR22725. The American Iron and Steel Institute provided technical assistance, construction materials and funding. Owens-Corning Corporation's Science and Technology Center provided additional technical assistance and construction materials.

References

- [1] 2001 ASHRAE Handbook Fundamentals, "Calculating Overall Thermal Resistance; Constructions Containing Metal; Zone Method of Calculation; Modified Zone Method for Metal Stud Walls with Insulated Cavities; Ceilings and Roofs," American Society of Heating, Refrigerating and Air-Conditioning Engineers, Inc., Atlanta, GA, 2001, pp. 23.8, 25.9-25.12.
- [2] Wilkes, K. E., Petrie, T. W., and Childs, P. W., "Precision and Bias of the Large Scale Climate Simulator in the Guarded Hot Box and Cold Box Modes," *Thermal Conductivity 23, Proceedings of the Twenty-Third International Thermal Conductivity Conference*, K. E. Wilkes, R. B. Dinwiddie and R. S. Graves, Eds., Technomic Publishing Company, Lancaster, PA, 1996, pp. 395-406.
- [3] Childs, K. W., "HEATING Users' Manual," Report ORNL/TM-12262, Oak Ridge National Laboratory, Oak Ridge, TN, 1993.
- [4] Steven Winter Associates, Inc., "Thermal Performance of Cold-Formed Steel Ceiling/Roof Framing Assemblies," Final Report on ASHRAE Research Project 981-TRP, Submitted to American Society of Heating, Refrigerating and Air-Conditioning Engineers, Inc., Atlanta, GA, July 1999.